J. Fluid Mech. (1968), *vol.* 32, *part* 4, *pp.* 681–692
Printed in Great Britain

Inclined buoyant puffs

By J. M. RICHARDS
Department of Electrical Engineering, Loughborough University of Technology

(Received 26 October 1967)

The motion of puffs which move in the direction of the buoyancy force was considered in a previous paper (Richards 1965). We now consider cases in which the directions of motion and of buoyancy are inclined or opposed. The main assumption is that the distributions of velocity inside the puffs are similar throughout the motion. Although this assumption is thought to be accurate only when the surroundings are neutral, we have reason to think that the same assumption may sometimes be used as an approximation to the internal distribution of velocity in other types of environment.

The particular case of motion when the buoyancy force is constant is calculated in detail. The calculations are supported by observations from new laboratory experiments.

1. Introduction

A puff is an isolated mass of strongly turbulent fluid which moves bodily through less turbulent surroundings. The interior and exterior fluids mix easily, and in consequence the size of the puff increases. The 'thermals' studied by Scorer (1957) and others are puffs of a type in which both the mean fluid motion and the internal turbulence are entirely generated by buoyancy forces. Later, Richards (1965) showed that several features of non-buoyant puffs in unstratified, non-turbulent, surroundings are apparently identical with the corresponding features of thermals. It was suggested that the only important effect of buoyancy in a puff is to change the impulse of the motion. The distributions of mean velocity and turbulence are substantially independent of buoyancy unless the densities of the interior and exterior fluids are very different.

Distributions of the mean fluid velocity inside and outside typical puffs in neutral surroundings have been measured by Miss Woodward (1959) and by the present author (Richards 1963, 1965). These distributions were observed to remain approximately similar throughout a substantial part of the motion. When the surroundings contained a sharp change of density at an interface between miscible fluids, Richards (1961) found that the gross motions of the puffs were not appreciably changed until the leading extremity of each puff reached the original level of the interface. Thus substantial changes in the distribution of external velocity can occur and yet affect the internal motions only slightly. The motions of puffs in neutral surroundings were also found to present many of the familiar features of vortex rings or vortex pairs (Lamb 1932). The mean

fluid motion and such characteristics of the turbulence as can be readily observed are roughly symmetrical about an axis (or plane). The force- and couple-resultants of the impulse of the vortex system then reduce to a single impulsive force along the line of symmetry in the direction of motion of the puff as a whole. The point at which the stream function is a maximum lies approximately on a maximum diameter of the puff normal to the line of symmetry, and so the intersection of such a diameter with this line moves through the surroundings with the velocity of the vortex system.

We here consider a more general type of motion, in which a buoyant or heavy puff may move at some appreciable angle to the vertical. It will be convenient to discuss concurrently cases in which the mean fluid motion is roughly symmetrical about an axis (axial puffs), or else is two-dimensional in a vertical plane (cylindrical puffs). We shall for brevity use a single symbol to represent, for example, the impulse I of an axial puff or the impulse per unit length I of a cylindrical puff, as appropriate.

2. Inclined puffs in unstratified surroundings

Figure 1 illustrates a puff which is moving at some angle, θ, to the horizontal. The main assumption of the present paper is that, in neutral surroundings, the distributions of mean and turbulent velocities in such a puff remain similar at all

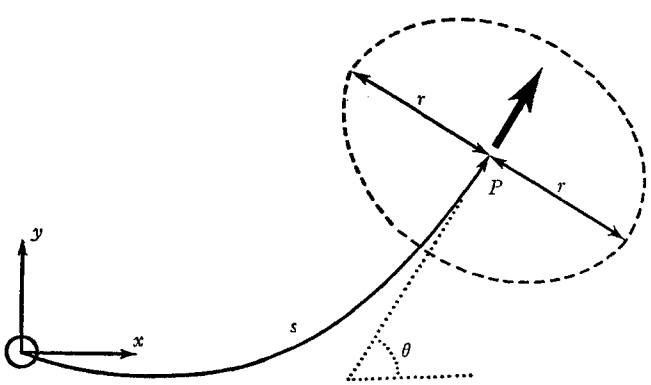

FIGURE 1. A puff, contained within the broken line, is subject to a buoyancy force parallel to Oy, and the central point P moves along a trajectory indicated by the full curve. The arc length, s, is measured from the virtual origin O to P.

stages of the motion. This assumption appears to be supported by the experimental results which will be presented later, and also by the observations which have been summarized in §1 above. The point P in figure 1, which is the intersection of the maximum diameter of the puff with the axis of symmetry of the mean motion, moves in the direction of the arrow. Let the speed of P be ds/dt; we take $ds/dt \geqslant 0$ without loss of generality. It has been explained, in §1, that the speed of P is approximately equal to the speed of the vortex system through its surroundings.

As the magnitude and direction of the impulse I varies through the operation of the buoyancy force, P moves along a trajectory which may be determined as follows.

Let the maximum diameter of the puff (figure 1) be $2r$. With the assumption of similarity, we have

$$r = ls, \tag{1}$$

where l is a positive constant which depends on the distributions of velocity. The point $r = s = 0$, is, of course, the virtual source of the puff.

Choosing rectangular Cartesian co-ordinates in the plane of the motion, we take the origin at the virtual source, with Ox parallel to the horizontal component of the initial impulse and Oy parallel to the initial direction of the buoyancy force. Resolving the impulse I into horizontal and vertical components, the momentum equations are, respectively,

$$\left.\begin{aligned} &(a)\ d(|I|\cos\theta)/dt = 0, \\ &(b)\ d(|I|\sin\theta)/dt = \pm|Mg|, \end{aligned}\right\} \tag{2}$$

where g is the gravitational acceleration and M is the difference between the masses contained within, and displaced by the puff. Generally,

$$M = M(t). \tag{3}$$

The sign on the right-hand side of (2) is positive whenever M has the same sign at the current time t and at the initial instant $t = 0$; otherwise the sign is negative. The negative sign may arise, for example, when the mixing of a volume of the fluid outside the puff with a volume of the internal fluid is accompanied by a change in the total volume. The mixing of ethanol and water may produce this result in liquids, and, in gases, such changes of volume follow, for example, the release or absorption of heat by condensation or evaporation of water droplets.

From the assumptions of similarity and the Boussinesq approximation, the magnitude of the impulse is given by

$$|I| = k\rho r^a(ds/dt), \tag{4}$$

where k is a positive constant, ρ is the mean density of the fluid, and $a = 2$ for a cylindrical puff or $a = 3$ for an axial puff.

Equations (1)–(4), with initial conditions

$$s = r = 0,\ |I| = I_0,\quad \theta = \theta_0,\quad t = 0, \tag{5}$$

allow one to calculate the trajectory of P when M is a given explicit or implicit function of time. An important example follows in §3.

3. Puffs of constant total buoyancy: trajectories

When Mg is constant, (2) may be integrated immediately, using the conditions (4), to give

$$\left.\begin{aligned} &(a)\ I_x = |I|\cos\theta = I_0\cos\theta_0 \\ &(b)\ I_y = |I|\sin\theta = I_0\sin\theta_0 + |Mg|\,t. \end{aligned}\right\} \tag{6}$$

It will be found helpful to recall that, if $\sin\theta$ is positive, the vertical component of the motion of P is in the direction of the buoyancy force.

If $I_x \neq 0$, we may divide (6b) by $I_0\cos\theta_0$ and use (6a), obtaining

$$\tan\theta = \tan\theta_0 + (|\mathrm{Mg}|/I_0\cos\theta_0)\,t. \tag{7}$$

Since the case $Mg = 0$ has already been investigated (Richards 1965), we now take $|Mg| > 0$. The cases in which $I_x = 0$ will be considered later in the present section.

From (7) we see that $\tan\theta$ may be used as a dimensionless measure of time unless $I_x = 0$. So let

$$\tan\theta = \tau, \quad \tan\theta_0 = \tau_0. \tag{8}$$

We define a dimensionless length scale, S, by

$$S^{a+1} = s^{a+1}\, 2|Mg|k\rho l^a/(a+1)\, I_0^2, \tag{9}$$

and since $ds/dt \geqslant 0$, and from (5), (9), we take

$$S \geqslant 0, \quad dS/dt \geqslant 0. \tag{10}$$

From (7) and (8), $$d\tau/dt = |Mg|/I_0 \cos\theta_0. \tag{11}$$

From (6a) and (8), $$|I| = I_0 \cos\theta_0 (1+\tau^2)^{\frac{1}{2}}. \tag{12}$$

To find an independent expression for $|I|$ we notice, from (1) and (4), that

$$(a+1)|I| = k\rho l^a\, d(s^{a+1})/dt. \tag{13}$$

That is, using (9) and (11),

$$2|I| = I_0 \sec\theta_0\, d(S^{a+1})/d\tau. \tag{14}$$

From (12) and (14), eliminating $|I|$,

$$\left.\begin{aligned} &(a)\ d(S^{a+1})/d\tau = 2\cos^2\theta_0 (1+\tau^2)^{\frac{1}{2}}, \\ &(b)\ \text{with boundary condition } S = 0 \text{ when } \tau = \tau_0. \end{aligned}\right\} \tag{15}$$

The solution of (15), which is facilitated by the substitution $\tau = \sinh\psi$, may be conveniently expressed in the form

$$\left.\begin{aligned} &(a)\ S^{a+1} = (F - F_0)\cos^2\theta_0, \\ \text{where}\quad &(b)\ F(\tau) = \sinh^{-1}\tau + \tau(1+\tau^2)^{\frac{1}{2}}, \\ \text{and}\quad &(c)\ F_0 = F(\tau_0). \end{aligned}\right\} \tag{16}$$

A graph of τ against F is shown in figure 2. From (16), $F(-\tau) = -F(\tau)$ and so only the first quadrant of the graph is shown. Figure 2 also shows the relation between F and θ implied by (16).

Equations (8) and (16) define the trajectory of P, and (7) defines the position of P on the trajectory as a function of time.

We next consider the various cases of vertical motion ($I_x = 0$), returning to (6b) in the form

$$I = (I_0 \sin\theta_0 + |Mg|t)/\sin\theta. \tag{17}$$

The case $I_0 = 0$ has already been considered (Richards 1965); the result is

$$s^{a+1} = (a+1)|Mg|t^2/2k\rho l^a. \tag{18}$$

When $I_0 \neq 0$, it is convenient to define a dimensionless time scale, T, by

$$T = |Mg|t/I_0. \tag{19}$$

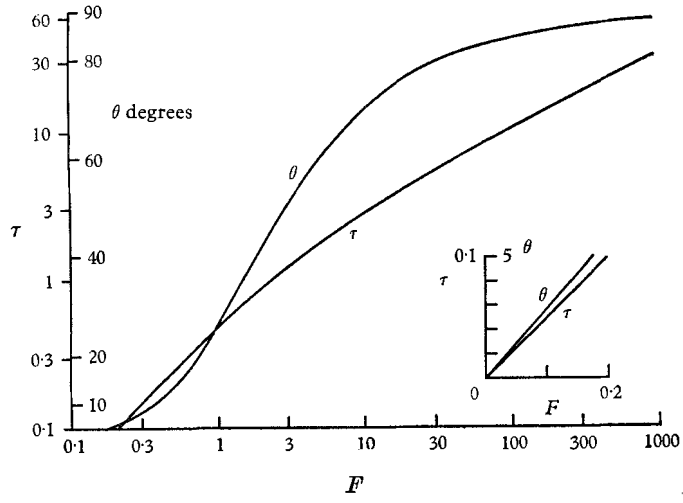

FIGURE 2. The function F defined by equation (16b). This function determines the shape of the trajectory of P, given the initial inclination θ_0, see (16a) and (9).

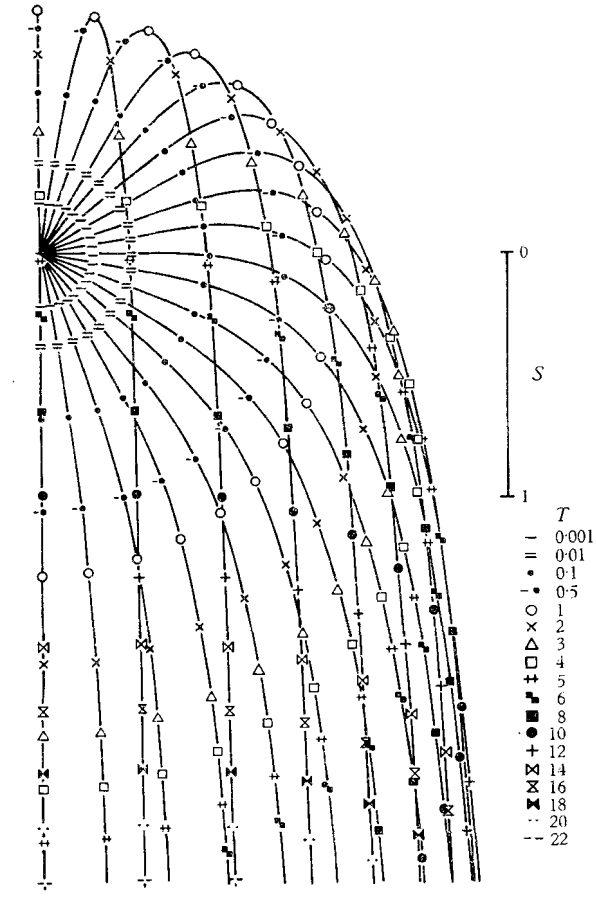

FIGURE 3. The trajectories of axial puffs at equal intervals (10 degrees) of the initial inclination θ_0, according to the assumptions of § 2.

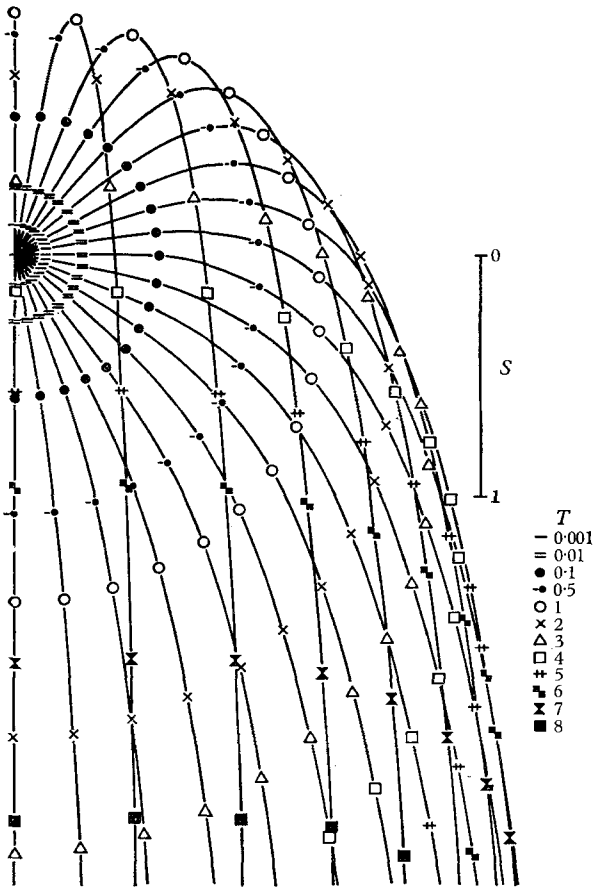

FIGURE 4. The trajectories of cylindrical puffs. This diagram may be compared with figure 3.

Proceeding as before, equation (15a) must be replaced by

$$d(S^{a+1})/dT = 2(\sin\theta_0 + T)/\sin\theta. \tag{20}$$

This equation may be integrated immediately, with appropriate constraints, to give solutions

$$S^{a+1} = T(2+T) \quad \text{for} \quad \sin\theta = \sin\theta_0 = +1, T \geqslant 0, \tag{21}$$

$$S^{a+1} = T(2-T) \quad \text{for} \quad \sin\theta = \sin\theta_0 = -1, 0 \leqslant T \leqslant 1, \tag{22}$$

$$S^{a+1} = 1+(T-1)^2 \quad \text{for} \quad \sin\theta = -\sin\theta_0 = +1, T > 1. \tag{23}$$

Figures 3 and 4 illustrate the expected trajectories of the puffs, according to the preceding theory. It can be seen that the motion when $T \ll 1$ is very much more rapid than when T is (0) 1. The greatest curvature always occurs when T is somewhat less than or equal to unity, that is to say when the increase of the vertical component of the impulse is roughly equal to the initial impulse.

4. Laboratory techniques

Some of the foregoing results have been verified in the laboratory. The experiments were performed in a rectangular water tank 1·5 m deep, 0·75 m wide and 2.1 m long. The apparatus, or puffer, which was used to produce axial puffs, is illustrated in figure 5. It consisted of a thick rigid cylindrical tube, capped at

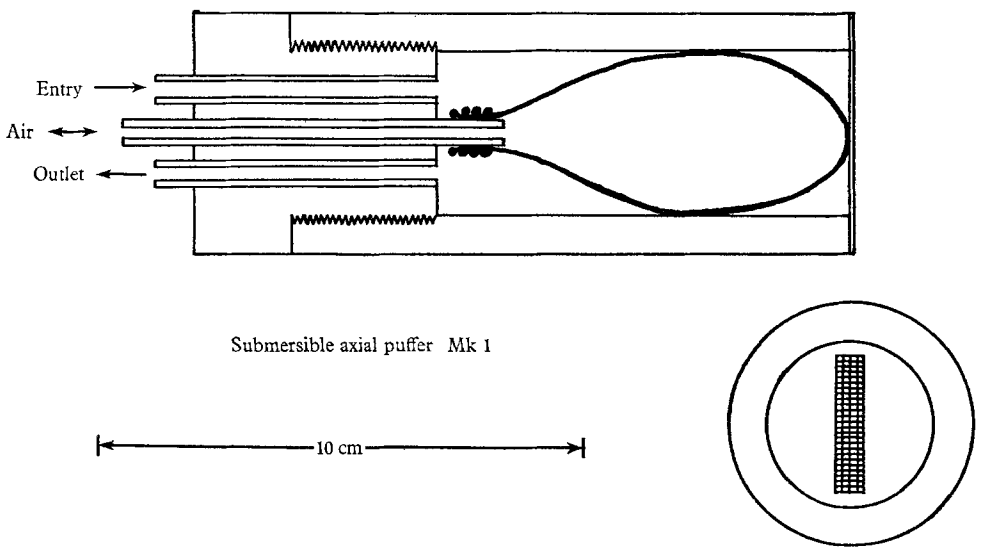

FIGURE 5. An apparatus used to produce inclined axial puffs, showing the rectangular orifice and the rubber balloon, which is in the partly inflated condition (§4).

one end by a thin disk having a rectangular orifice which was covered by a coarse wire mesh. A screwed plug closed the base of the puffer. The plug was penetrated by three small tubes which were connected by flexible rubber tubing, through the free surface of the water in the experimental tank, to the other apparatus in the laboratory. A supply of air at a variable pressure was used to inflate and deflate a rubber balloon which was tied by its neck to the inner end of the central tube. One of the outer tubes was used to supply a mixture of solutions of a dye and of sodium chloride in water, the density of the mixture was 1·15 g cm^{-3}. The remaining tube was used to convey liquid to waste.

In operation, the puffer was first submerged and tilted to and fro in order to remove bubbles of air. The orifice disk was then attached to the open end by an internally threaded and flanged collar. The puffer was clamped at the desired inclination and at about 20 cm below the free surface. The balloon was partly inflated, as shown in figure 5, where it will be seen that a body of fluid at the plugged end, or 'base', was then disconnected from the main body of water in the tank.

The dyed mixture was then introduced through the plug, and an equal volume of fluid was removed to waste, until the base of the puffer contained substantially undiluted dyed mixture.

When a puff was required, the supply and waste mixture pipes were closed

and the balloon was rapidly deflated. A quantity of water rushed in through the orifice and mixed with the fluid from the base of the puffer. As soon as dyed liquid was seen to emerge from the orifice, the balloon was suddenly and fully inflated, and so a cloud of dense dyed liquid was forced into the tank. Due to the rectangular shape of the orifice, an axial puff developed. A vortex ring would have been expected if the orifice had been roughly circular (Richards 1965).

The motion of the puff was recorded on ciné film, using a shadowgraph technique. The readings of a clock, which registered to 0·01 sec, were recorded on the same film. A sequence of enlargements from the film of a particular experiment is shown in figure 6, plate 1. It was found that the axial puff was always followed by a considerable mass of dyed fluid in the form of a tail or wake, and this tail must sometimes have contained significant fractions of the mass and momentum ejected by the puffer. Although subsidiary puff motions often developed in the tail, the motion of the main puff appeared to be almost independent of the motion developed by the tail if the angle of projection, θ_0, was greater than about $-20°$. This independence is not surprising when we recall Woodward's (1959) results, which show that the speed of the fluid motion surrounding an isolated axial puff decreases rapidly with distance from the centre of the puff. In order to avoid appreciable interference by the tail and yet to produce trajectories which display substantial variation of θ during the course of an experiment, the main experiments were conducted with the axis of the puffer near the horizontal.

Besides these experiments with axial puffs, some observations were made of cylindrical puffs which were projected almost directly against the buoyancy force. The apparatus in these cases was the cylindrical puffer previously described (Richards 1965), which was now set at an angle of about 10° to the vertical (i.e. $\theta_0 \simeq -80°$). This puffer was filled with a dyed buoyant mass of a dilute solution of ethyl alcohol in water. Unfortunately, the method requires that the free surface of the water in the tank is fairly close to the level of the puffer orifice, and consequently the observations could not be continued far beyond the culminating point of each trajectory.

5. Experimental results

The ciné film of each experiment was projected frame by frame and silhouettes of the puff were traced on to a single sheet of paper. Two fiducial marks on the front wall of the tank were used to ensure the same registration and enlargement throughout, so that the traced silhouettes depicted successive stages in the motion relative to the laboratory. The reading of the clock corresponding to each silhouette was also taken, this time will be denoted by $(t-t_1)$. A transparent rule was used to estimate the centre of each silhouette, the locus of this centre is the

---

FIGURE 6 (opposite). A sequence from ciné film, showing successive stages in the motion of a dense axial puff, made visible in water with a black dye and a shadowgraph. Each photograph appears with the corresponding number of ciné frames since the puff began to emerge from the puffer. Filming speed 18 frames per second. The free surface appears as a dark line near the top of each photograph; the small black fixed marks were 30 cm apart. The photographs show only the upper central portion of the large experimental tank.

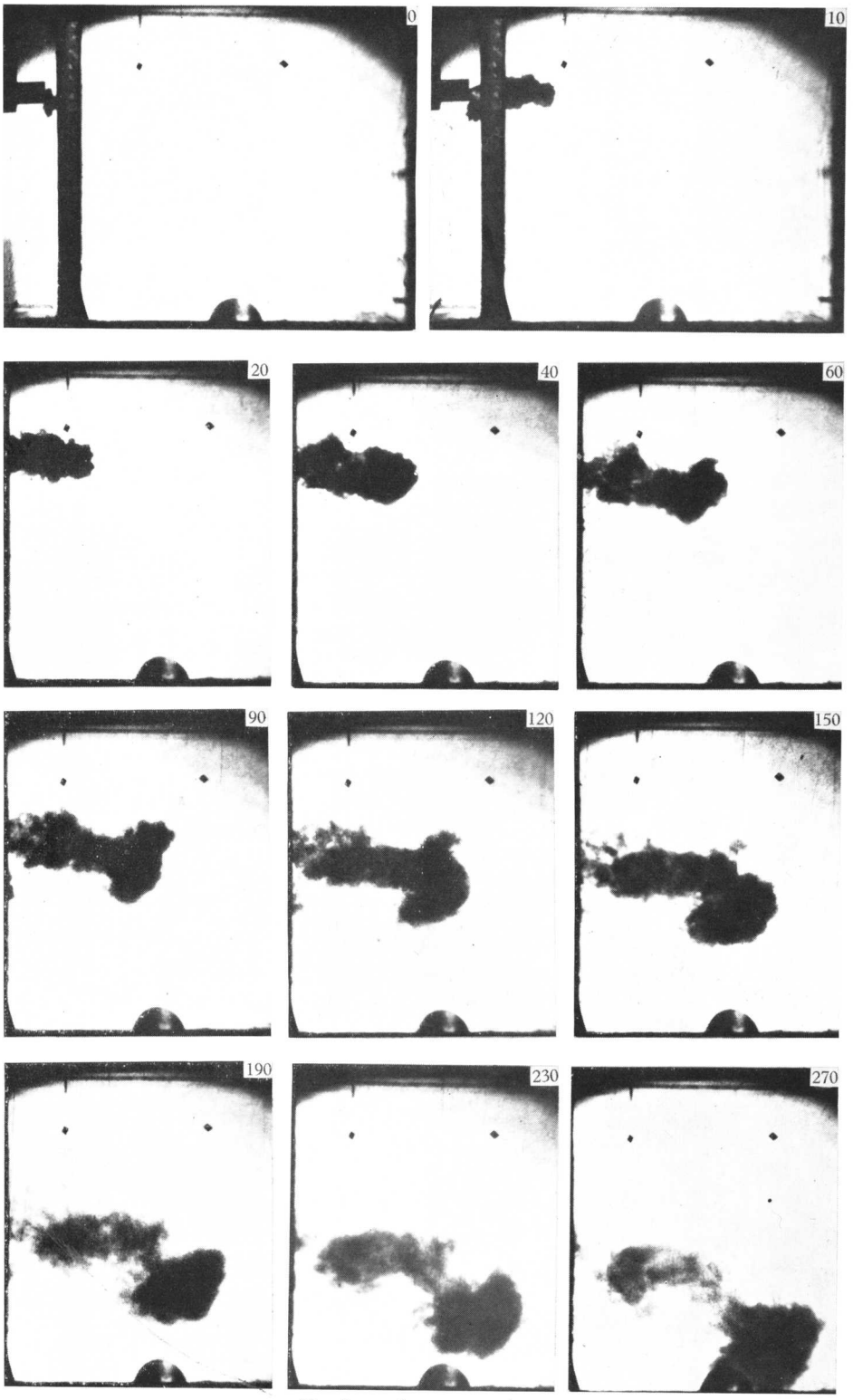

For legend see opposite.

(*Facing p.* 688)

trajectory of the point P of figure 1. Typical silhouettes, with loci, are shown in figure 7.

Corresponding values of the diameter $2r$, and of the arc length along the estimated trajectory of P from some arbitrary fixed origin, which we shall denote by

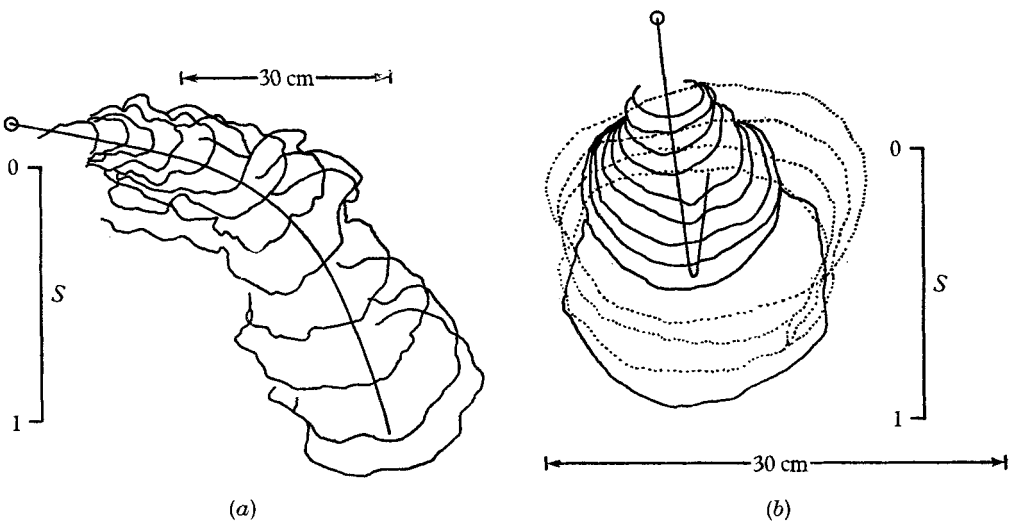

FIGURE 7. The silhouettes of puffs, traced from enlargements of ciné photographs. An estimate of the trajectory of the central point P (figure 1) is superimposed, and the estimated position of the virtual origin is indicated by O. (*a*) shows an axial puff, (*b*) a cylindrical puff.

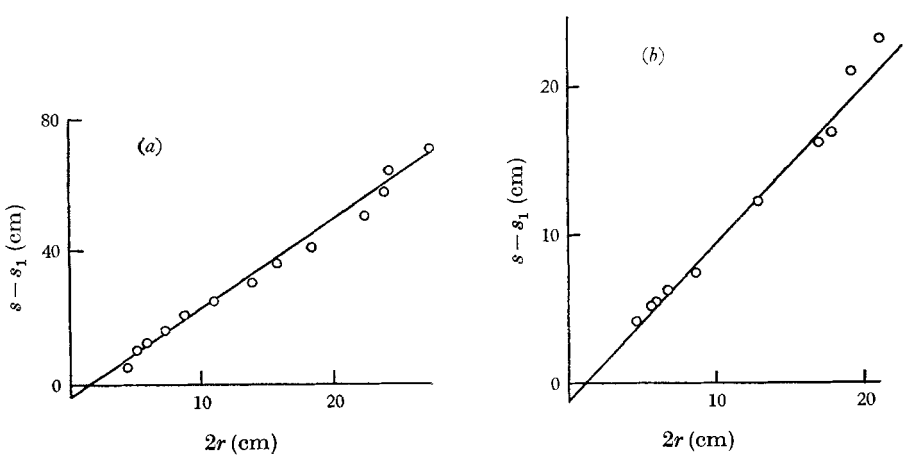

FIGURE 8. Typical graphs of the arc displacement, $(s-s_1)$, against the diameter, $2r$, for (*a*) an axial puff and (*b*) a cylindrical puff.

$(s-s_1)$, were measured from each silhouette. The measuring wheel of a planimeter was particularly convenient for the latter measurement, which was taken round a curve. Graphs of $(s-s_1)$ against $2r$, such as those shown in figure 8, indicate that the value of l, equation (1), is roughly constant throughout each motion, in agreement with the assumption made. The value of s_1 was measured

from the intercept on the graph, and thence the virtual origin of the motion was marked on the estimated trajectory.

The values of l obtained obtained in these experiments, as well as the shapes of the puff silhouettes (so far as these could be clearly distinguished from their tails) are consistent with those obtained in earlier work.

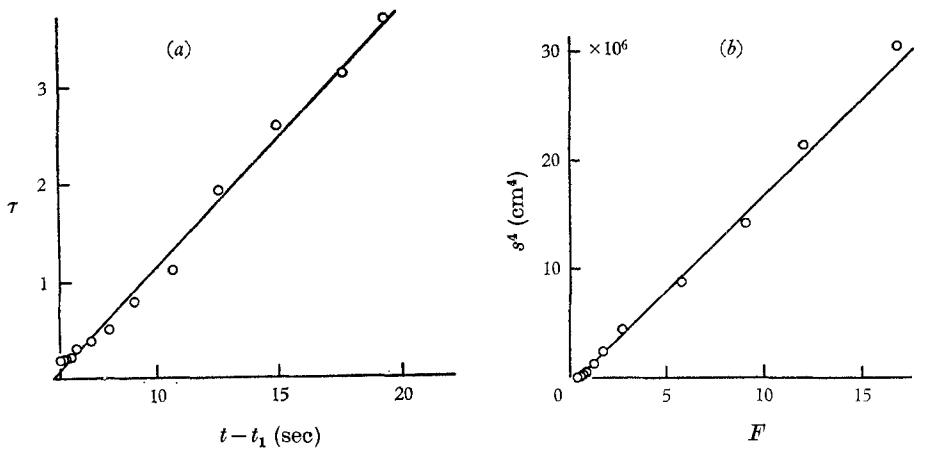

FIGURE 9. These graphs relate to an axial puff. (*a*) A typical graph of slope, τ, against indicated time, $(t-t_1)$, verifying (7). (*b*) A typical graph of s^4 against F, verifying (16*a*).

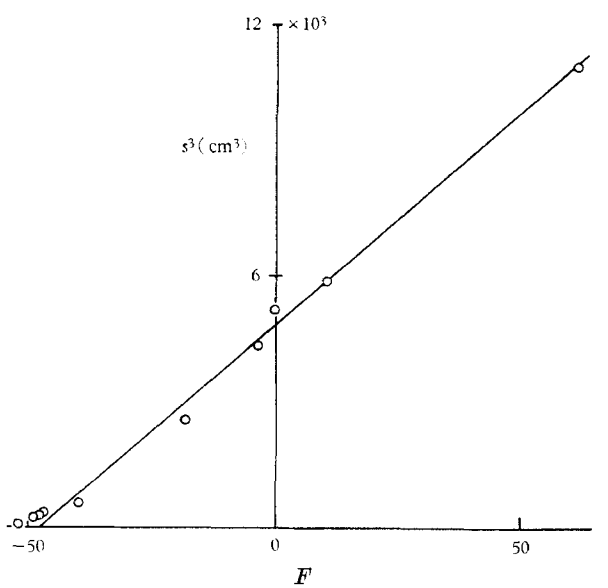

FIGURE 10. A typical graph of s^3 against F, for a cylindrical puff, verifying (16*a*).

Figure 9(*a*) shows a graph of τ against the time $(t-t_1)$, in the case of an axial puff. Each value of $\tau = \tan\theta$ was obtained by measuring θ on the estimated trajectory of a silhouette diagram like figure 7(*a*). Figure 9(*a*) shows that τ varies linearly with t, in agreement with equation (7).

The measured values of τ were used to calculate corresponding values of F, equation (16*b*). We see from equations (16*a*) and (9) that s^{a+1} should be directly proportional to $(F-F_0)$, and this result was verified by graphs of s^4 against F, such as figure 9(*b*). The intercept on the axis of F gave an estimate of F_0, which was used to calculate τ_0, and so θ_0, using (16) and (8). Such calculations have been used to revise an initial estimate of the trajectory in figure 7(*a*). It was observed that the axial puffer often projected puffs at an appreciable angle to its axis; perhaps this effect was associated with unwanted variations in the operation of the rubber balloon.

Since the experiments with cylindrical puffs were always associated with values of θ_0 close to -80 degrees, only a few values of τ could be measured accurately, and so (7) could not be verified directly in the manner of figure 9(*a*). Accordingly, (7) was assumed, and only the initial value τ_0 was measured from the trajectory. The constant of proportionality in (7) is equal to the ratio of τ_0 to the interval of time between $t = 0$ and the instant when the trajectory becomes horizontal. This interval was estimated directly, though approximately, from the ciné film. The initial clock reading, $-t_1$, was estimated in the same way. The observed values of $(t-t_1)$ were then converted, using (7), into corresponding values of τ. The procedure was then completely analogous to that used for axial puffs and described in the preceding paragraph. As shown in figure 10, the resulting graph of s^3 against F is roughly linear, in agreement with (16*a*) and (9).

6. Suggestions and conclusions

A self-preserving turbulent flow, such as has been assumed in the present paper, can only be expected when the Reynolds number $R = (r\,ds/dt)/\nu$, exceeds some critical value. If the motion on some part of a trajectory (figures 3, 4) causes the value of R to become less than this, the motion may be expected to change, though perhaps only gradually, towards some less turbulent form such as a vortex ring or vortex pair. Later, the continued action of the buoyancy force may cause R to increase until puff motion is resumed. This second critical value of R may be greater than the first, and the critical values may depend on other properties of the motions, such as the circulation. The detailed examination of these suggestions is beyond the scope of the present paper.

The experimental results of § 7 agree closely with the corresponding theoretical predictions, and so provide considerable support for the assumptions made in § 2. The same assumptions can accordingly be expected to be generally useful whenever the Reynolds number R remains sufficiently large.

I wish to thank Mr J. Rippon and Miss W. Foley (now Mrs Bo) for their assistance with the experimental work. Mrs Bo received support from the British Meteorological Office.

REFERENCES

LAMB, H. 1932 *Hydrodynamics*, 6th edn. Cambridge University Press.

RICHARDS, J. M. 1961 Experiments on the penetration of an interface by buoyant thermals. *J. Fluid Mech.* **11**, 369–84.

RICHARDS, J. M. 1963 Experiments on the motions of isolated cylindrical thermals through unstratified surroundings. *Int. J. Air Water Pollution*, **7**, 17–34.

RICHARDS, J. M. 1965 Puff motions in unstratified surroundings. *J. Fluid Mech.* **21**, 97–106.

SCORER, R. S. 1957 Experiments on convection of isolated masses of buoyant fluid. *J. Fluid Mech.* **2**, 583–94.

WOODWARD, B. 1959 The motion in and around isolated thermals. *Quart. J. Roy. Met. Soc.* **85**, 144–51.